

Nambu Monopoles in Lattice Electroweak Theory

B.L.G.Bakker

Department of Physics and Astronomy, Vrije Universiteit, Amsterdam, The Netherlands.

E-mail: blg.bakker@few.vu.nl

A.I.Veselov

ITEP, B.Chermushkinskaya 25, Moscow, 117259, Russia.

E-mail: veselov@itep.ru

M.A.Zubkov

ITEP, B.Chermushkinskaya 25, Moscow, 117259, Russia.

E-mail: zubkov@itep.ru

Abstract. We considered the lattice electroweak theory at realistic values of α and θ_W and for large values of the Higgs mass. We investigated numerically the properties of topological objects that are identified with quantum Nambu monopoles. We have found that the action density near the Nambu monopole worldlines exceeds the density averaged over the lattice in the physical region of the phase diagram. Moreover, their percolation probability is found to be an order parameter for the transition between the symmetric and the broken phases. Therefore, these monopoles indeed appear as real physical objects. However, we have found that their density on the lattice increases with increasing ultraviolet cutoff. Thus we conclude, that the conventional lattice electroweak theory is not able to predict the density of Nambu monopoles. This means that the description of Nambu monopole physics based on the lattice Weinberg - Salam model with finite ultraviolet cutoff is incomplete. We expect that the correct description may be obtained only within the lattice theory that involves the description of TeV - scale physics.

PACS numbers: 12.15.-y, 11.15.Ha, 12.10.Dm

1. Introduction

The electroweak theory does not contain topologically stable monopole-like objects. However, certain unstable objects of topological nature still exist in this theory. One of the examples is the so-called Nambu monopole[1]. It must be connected by the so-called Z string with the corresponding antimonopole. The Z string has nonzero tension. Therefore only the monopole - antimonopole bound state may appear as an observable object. The mass of the Nambu monopole (realized as a classical field configuration) was estimated to be of the order of several TeV. This is not far from the energies that may be achieved by modern colliders, in particular, the LHC. Thus one may suppose, that an indication of its existence may be detected in the near future.

Nambu monopoles are not described by means of a perturbation expansion around the trivial vacuum background. Therefore, nonperturbative methods should be used in order to investigate their physics. Lattice methods seem to be one of the ways to deal with Nambu monopoles. It should be stressed that the mass of the Nambu monopole is close to the energy scale, where (as commonly believed) the Standard Model does not work[2, 3]. This creates an additional difficulty while considering the problem.

Qualitative lattice investigations of the properties of Nambu monopoles in the Standard Model have been performed both at zero and finite temperature in the unphysical region of large coupling constants [4, 5, 6, 7]. Nambu monopoles were found to be condensed in the symmetric phase of lattice theory (and above the electroweak transition in the finite temperature theory). In the present paper we continue this investigation for realistic values of the renormalized coupling constants ($\alpha \sim 1/128$ and $\theta_W = \pi/6$) within the zero temperature theory. It should be stressed that originally Nambu monopoles were defined as classical objects[1]. Therefore there could appear several lattice definitions of *quantum* Nambu monopoles. In this paper we discuss two of them and investigate the difference between the positions of the corresponding monopole trajectories.

The numerical investigation of Gauge-Higgs models has a long history. First studies of nonabelian Gauge-Higgs systems were performed in eighties and were devoted mainly to the investigation of $SU(2)$ Gauge-Higgs model at zero temperature (see, for example, [8, 9, 10, 11, 12] and references therein). In these studies the general phase structure of the model was established. At small values of the scalar self coupling λ the first order phase transition between the physical Higgs phase and the unphysical symmetric phase of the model was found. The phase transition becomes weaker as λ is increased. Using the weak coupling expansion [13] it was found that the maximal value of the ultraviolet cutoff in the theory is achieved at infinite λ . At $\lambda \rightarrow \infty$ also the absolute upper bound on the Higgs boson mass is achieved which was found to be of the order of $10M_W$ (see, for example, [10, 11, 12]). An early study of the $SU(2) \otimes U(1)$ Gauge-Higgs model was performed in [14], where the phase diagram of the model was given. In general, the description of the phase diagram is similar to that of given in the present paper (see Fig. 1, and discussion in section 5.1).

Table 1. The values of the cutoff used in some selected lattice studies of the $SU(2)$ Gauge - Higgs model.

Reference	ultraviolet Cutoff (GeV)	M_H (GeV)
[15]	140 (space direction) 570 (time direction)	80
[16]	280 (time direction)	80
[17]	280	34
[18]	110	16
[19]	90 (space direction) 350 (time direction)	34
[20]	280	48
[21]	140	35
[22]	280	20 , 50
[23]	190	50
[24]	260	57 - 85
[25]	200 - 300	47 - 108
[10]	400	480
[11]	330 - 470	280 - 720 (both $\lambda = \infty$ and finite λ)
[12]	250 - 470	720 (both $\lambda = \infty$ and finite λ)

The next step in the numerical investigation of Gauge-Higgs models was motivated by an attempt to explore the physics of finite temperature electroweak phase transition and its relation to cosmology, in particular, to the problem of baryon asymmetry (see, for example, [15, 16, 17, 18, 19, 20, 21, 22, 23, 24, 25, 26] and references therein). One of the achievements of these studies was that the endpoint of the phase transition line (in the $T - M_H$ plane) was found. It was found that at the experimentally allowed values of the Higgs mass the transition in the standard electroweak theory is a crossover.

In $4D$ lattice studies of $SU(2)$ Gauge-Higgs theory the scale is fixed by the value of the W -boson mass. Namely, the mass measured in lattice units is $M_W = a \times 80 \text{ Gev}$, where a is the value of the lattice spacing. The ultraviolet cutoff is $\Lambda = \frac{1}{a}$. In Table 1 we summarize the data on the ultraviolet cutoff used in selected lattice studies of the $SU(2)$ Gauge-Higgs model. In all these studies the coupling constant corresponding to the fine structure constant of the Weinberg-Salam model is around $\alpha \sim 1/100$. The potential for the Higgs boson was used with different values of λ .

The numerical investigation of the monopole-like [27] and string - like topological objects in Abelian Gauge-Higgs systems has also a long history (see, for example, [28]). For an early study of the percolation of monopole currents see [29]. It has been found that the monopole density drops sharply to zero in the Coulomb phase of the model while in the confining phase it is nonzero. The vortex density is nonzero in the Coulomb phase and drops to zero in the Higgs phase. The situation with topological defects in nonabelian Gauge-Higgs systems is in general similar to that of the Abelian ones. The

first numerical investigation of topological defects in 3D lattice $SU(2)$ Gauge-Higgs model (corresponding to finite temperatures) was performed in [30]. It was found that the percolation of Z -vortices is the order parameter for the electroweak transition. The conjecture that Nambu-monopole percolation feels the electroweak transition was made first in [31].

In our earlier papers we considered the appearance of an additional discrete symmetry in the fermion sector of the Standard Model[4, 5, 6, 7]. This additional symmetry allows to define the Standard Model with the gauge group $SU(3) \times SU(2) \times U(1)/\mathcal{Z}$, where \mathcal{Z} is equal to Z_6 , or to one of its subgroups: Z_3 or Z_2 . It is worth mentioning that it has been recognized much earlier that the Standard Model appears with the gauge group $SU(3) \times SU(2) \times U(1)/Z_6$ as a result of the spontaneous breakdown in the $SU(5)$ unified model[32]. Independently, the Z_6 symmetry in the Higgs sector of the Standard Model was considered in [33].

In the present paper we use two lattice realizations of the electroweak theory: with the gauge groups $SU(2) \times U(1)/Z_2$, and $SU(2) \times U(1)$, respectively. The $SU(2) \times U(1)/Z_2$ model should be the part of the Standard Model with the gauge group $SU(3) \times SU(2) \times U(1)/Z_2$ or $SU(3) \times SU(2) \times U(1)/Z_6$, while the $SU(2) \times U(1)$ model could be the part of the Standard Model with the gauge group $SU(3) \times SU(2) \times U(1)/Z_3$ or $SU(3) \times SU(2) \times U(1)$. We comment on the difference between the two lattice models, which appears in our numerical research in the unphysical region with a large coupling constant.

The paper is organized as follows. In Sect. 2 we describe the lattice models under consideration. In Sect. 3 we present the definition and the main properties of quantum Nambu monopoles. Sect. 4 contains our description of the quantities to be measured. In Sect. 5 we report our main numerical results, while in Sect. 6 we discuss the difference between the two versions of the lattice electroweak model. The final section contains our conclusions.

2. Lattice models under investigation

In this section we describe the lattice models under consideration. We do not consider the color sector of the Standard Model. Therefore, we are left with two possibilities: the gauge groups $SU(2) \times U(1)/Z_2$, and $SU(2) \times U(1)$. We also neglect dynamical fermions. In both cases we use the following lattice variables:

1. The gauge field $\mathcal{U} = (U, \theta)$, where

$$U = \begin{pmatrix} U^{11} & U^{12} \\ -[U^{12}]^* & [U^{11}]^* \end{pmatrix} \in SU(2), \quad e^{i\theta} \in U(1), \quad (1)$$

are realized as link variables.

2. A scalar doublet

$$\Phi_\alpha, \quad \alpha = 1, 2. \quad (2)$$

The potential for the scalar field is considered in its simplest form [5] in the London limit, i.e., in the limit of infinite bare Higgs mass. In the lattice study this does not mean, however, that the physical Higgs mass is infinite[9]. Instead we expect only that it should not be less than the inverse lattice spacing. This is indeed confirmed via direct calculation. From the very beginning we fix the unitary gauge $\Phi_1 = \sqrt{\gamma}$, $\Phi_2 = 0$.

For the case of the $SU(2) \times U(1)/Z_2$ symmetric model we chose the action of the form

$$S_g = \beta \sum_{\text{plaquettes}} \left((1 - \frac{1}{2} \text{Tr } U_p \cos \theta_p) + \frac{1}{2} (1 - \cos 2\theta_p) \right) + \gamma \sum_{xy} (1 - \text{Re}(U_{xy}^{11} e^{i\theta_{xy}})), \quad (3)$$

where the plaquette variables are defined as $U_p = U_{xy} U_{yz} U_{wz}^* U_{xw}^*$, and $\theta_p = \theta_{xy} + \theta_{yz} - \theta_{wz} - \theta_{xw}$ for the plaquette composed of the vertices x, y, z, w .

For the case of the conventional $SU(2) \times U(1)$ symmetric model we use the action

$$S_g = \beta \sum_{\text{plaquettes}} \left((1 - \frac{1}{2} \text{Tr } U_p) + 3(1 - \cos \theta_p) \right) + \gamma \sum_{xy} (1 - \text{Re}(U_{xy}^{11} e^{i\theta_{xy}})). \quad (4)$$

In both cases the bare Weinberg angle is $\theta_W = \pi/6$, which is close to its experimental value. The renormalized Weinberg angle is to be calculated through the ratio of the lattice masses: $\cos \theta_W = M_W/M_Z$. The bare fine structure constant α is expressed through β as $\alpha = 1/4\pi\beta$. However, the renormalized coupling extracted from the potential for infinitely heavy fermions differs from this simple expression, as will be shown in the next sections. The physical meaning of the constant γ is that it is equal to the square of the vacuum value of Φ_1 .

The following variables are considered as creating a Z boson and a W boson, respectively:

$$\begin{aligned} Z_{xy} &= Z_x^\mu = \sin [\text{Arg} U_{xy}^{11} + \theta_{xy}], \\ W_{xy} &= W_x^\mu = U_{xy}^{12} e^{-i\theta_{xy}}. \end{aligned} \quad (5)$$

Here, μ represents the direction (xy) .

After fixing the unitary gauge the electromagnetic $U(1)$ symmetry remains:

$$\begin{aligned} U_{xy} &\rightarrow g_x^\dagger U_{xy} g_y, \\ \theta_{xy} &\rightarrow \theta_{xy} - \alpha_y/2 + \alpha_x/2, \end{aligned} \quad (6)$$

where $g_x = \text{diag}(e^{i\alpha_x/2}, e^{-i\alpha_x/2})$.

In the unitary gauge there is also a $U(1)$ lattice gauge field, which is defined as

$$A_{xy} = A_x^\mu = [-\text{Arg} U_{xy}^{11} + \theta_{xy}] \text{ mod } 2\pi, \quad (7)$$

The fields A , Z , and W transform as follows:

$$\begin{aligned} A_{xy} &\rightarrow A_{xy} - \alpha_y + \alpha_x, \\ Z_{xy} &\rightarrow Z_{xy}, \\ W_{xy} &\rightarrow W_{xy} e^{-i\alpha_x}. \end{aligned} \quad (8)$$

It should be mentioned that the field A cannot be treated as the usual electromagnetic field, because the set of variables A , Z , and W do not diagonalize the kinetic part of the pure gauge action in its naive continuum limit. In our lattice model the electromagnetic field A_{EM} should be defined as

$$A_{\text{EM}} = A + Z' - 2 \sin^2 \theta_W Z', \quad (9)$$

where $Z' = [\text{Arg}U_{xy}^{11} + \theta_{xy}] \text{mod} 2\pi$.

3. Nambu monopoles

First, we define the continuum electroweak fields as they appear in the Weinberg-Salam model in the way appropriate for the topological consideration. Namely, after fixing the unitary gauge $\Phi_1 = \text{const.}$, $\Phi_2 = 0$, where Φ is the scalar field of the electroweak theory, the Z -boson field Z^μ and electromagnetic field A_{EM}^μ are defined as

$$\begin{aligned} Z^\mu &= \frac{1}{2} \text{Tr} C^\mu \sigma_3 + B^\mu, \\ A_{\text{EM}}^\mu &= 2B^\mu - 2 \sin^2 \theta_W Z^\mu, \end{aligned} \quad (10)$$

where C^μ and B^μ are the corresponding $SU(2)$ and $U(1)$ gauge fields of the Standard Model.

Nambu monopoles are defined as the endpoints of the so-called Z -string [1]. The Z -string is the classical field configuration that represents an unstable object, which is characterized by the magnetic flux extracted from the Z -boson field. Namely, for a small contour \mathcal{C} winding around the Z -string one should have

$$\int_{\mathcal{C}} Z^\mu dx^\mu \sim 2\pi; \quad \int_{\mathcal{C}} A_{\text{EM}}^\mu dx^\mu \sim 0; \quad \int_{\mathcal{C}} B^\mu dx^\mu \sim 2\pi \sin^2 \theta_W. \quad (11)$$

The string terminates at the position of the Nambu monopole. The hypercharge flux is supposed to be conserved at that point \ddagger . Therefore, a Nambu monopole carries electromagnetic flux $4\pi \sin^2 \theta_W$. The size of Nambu monopoles was estimated [1] to be of the order of the inverse Z -boson mass, while its mass should be of the order of a few TeV. According to [1] Nambu monopoles may appear only in the form of a bound state of a monopole-antimonopole pair.

In lattice theory the classical solution corresponding to a Z -string should be formed around the 2-dimensional topological defect which is represented by the integer-valued field defined on the dual lattice

$$\Sigma = \frac{1}{2\pi}^* ([dZ']_{\text{mod} 2\pi} - dZ') \quad (12)$$

(Here we used the notations of differential forms on the lattice. For a definition of those notations see, for example, [34].) Therefore, Σ can be treated as the worldsheet of a *quantum* Z -string[31, 7, 30].

\ddagger On the classical level the monopole - like topological objects with nontrivial hypercharge flux have an infinite self energy. At the quantum level such objects are present in the lattice theory at the finite values of lattice spacing. However, in the physically interesting region of lattice coupling constant $\beta \sim 15$ the density of these objects vanishes (see Section 6 of the present paper).

Then, worldlines of quantum Nambu monopoles appear as the boundary of the Z -string worldsheet:

$$j_Z = \delta\Sigma \quad (13)$$

It has been mentioned in the previous section that our lattice models become $U(1)$ gauge models after fixing the unitary gauge. The corresponding compact $U(1)$ gauge field is given by Eq. (7). Therefore one may try to extract monopole trajectories directly from A . Actually this was done in our earlier papers [4, 5, 6, 7]. The monopole current is given by

$$j_A = \frac{1}{2\pi} *d([dA] \bmod 2\pi) \quad (14)$$

Both j_Z and j_A represent objects carrying magnetic charge. Therefore it would be instructive to reveal the correspondence between them. We have

$$A = [-Z' + 2\theta] \bmod 2\pi. \quad (15)$$

In continuum notation this would be

$$A^\mu = -Z^\mu + 2B^\mu, \quad (16)$$

where B is the hypercharge field. Its strength is divergenceless. As a result in continuum theory the net Z flux emanating from the center of the monopole is equal to the net A flux with the opposite sign. (Both A and Z are undefined inside the monopole.) This means that in the continuum limit the position of the Nambu monopole must coincide with the position of the antimonopole extracted from the field A . Therefore, one can consider Eq. (14) as another definition of a quantum Nambu monopole. It is interesting that the definition (14) is not directly related to any observable string, as the Dirac string connecting the corresponding lattice monopoles is invisible.

4. Quantities to be measured

4.1. Evaluation of the lattice spacing

The physical scale is given in our lattice theory by the value of the Z -boson mass $M_Z^{\text{phys}} \sim 90$ GeV. Therefore the lattice spacing is evaluated to be $a \sim [90 \text{ GeV}]^{-1} M_Z$, where M_Z is the Z boson mass in lattice units.

In order to evaluate the mass of the Z -boson we use the correlator [9]:

$$\sum_{\bar{x}, \bar{y}} \langle \sum_{\mu} Z_x^\mu Z_y^\mu \rangle \sim e^{-M_Z |x_0 - y_0|} + e^{-M_Z (L - |x_0 - y_0|)}, \quad (17)$$

Here the summation $\sum_{\bar{x}, \bar{y}}$ is over the three ‘‘space’’ components of the four - vectors x and y while x_0, y_0 denote their ‘‘time’’ components. L is the lattice length in the ‘‘time’’ direction.

It is worth mentioning, that in the Z -boson channel many photon states also exist. The mass of the corresponding state on the finite lattice we used is, however, larger than that of the Z - boson itself. For example, on the lattice $16^3 \times 24$ the minimal mass

of the 3 - photon state is $M_{3\gamma} = 2\frac{2\pi}{16} + \frac{4\pi}{16} \sim 1.5$. Moreover, from the point of view of perturbation theory this state appears in the correlator (17) through a virtual loop and is suppressed by the factor α^3 .

4.2. The Higgs boson mass.

The Higgs boson mass in lattice units is measured using the correlator

$$\sum_{\bar{x}, \bar{y}} (\langle H_x H_y \rangle - \langle H \rangle^2) \sim e^{-M_H |x_0 - y_0|} + e^{-M_H (L - |x_0 - y_0|)}, \quad (18)$$

where H is the Higgs boson creation operator.

We used three different operators that create Higgs bosons:

$$H_x = \sum_y |W_{xy}|^2, \quad (19)$$

$$H_x = \sum_y Z_{xy}^2 \quad (20)$$

and

$$H_x = \sum_y \text{Re}(U_{xy}^{11} e^{i\theta_{xy}}) \quad (21)$$

Here H_x is defined at the site x , the sum \sum_y is over its neighboring sites y .

4.3. The renormalized coupling

The bare constant $\alpha = e^2/4\pi$ (where e is the electric charge) can be easily calculated in our lattice model. It is found to be equal to $1/(4\pi\beta)$. Therefore, its physical value $\alpha(M_Z) \sim 1/128$ could be achieved at values of β in the vicinity of 10. This naive guess is, however, to be corrected by the calculation of the renormalized coupling constant α_R . We perform this calculation using the potential for infinitely heavy external fermions. We consider Wilson loops for the right-handed external leptons:

$$\mathcal{W}_{\text{lept}}^{\text{R}}(l) = \langle \text{Re} \Pi_{(xy) \in l} e^{2i\theta_{xy}} \rangle. \quad (22)$$

Here l denotes a closed contour on the lattice. We consider the following quantity constructed from the rectangular Wilson loop of size $r \times t$:

$$\mathcal{V}(r) = \log \lim_{t \rightarrow \infty} \frac{\mathcal{W}(r \times t)}{\mathcal{W}(r \times (t+1))}. \quad (23)$$

Owing to the exchange of virtual photons at large distances we expect the appearance of the Coulomb interaction

$$\mathcal{V}(r) = -\frac{\alpha_R}{r} + \text{const}. \quad (24)$$

It should be mentioned here, that in order to extract the renormalized value of α one may apply to \mathcal{V} the fit obtained using the Coulomb interaction in momentum space. The lattice Fourier transform then gives

$$\begin{aligned} \mathcal{V}(r) &= -\alpha_R \mathcal{U}(r) + \text{const}, \\ \mathcal{U}(r) &= \frac{\pi}{L^3} \sum_{\vec{p} \neq 0} \frac{e^{ip_3 r}}{\sin^2 p_1/2 + \sin^2 p_2/2 + \sin^2 p_3/2} \end{aligned} \quad (25)$$

Here L is the lattice size, $p_i = \frac{2\pi}{L}k_i$, $k_i = 0, \dots, L-1$. On large enough lattices at $r \ll L$ both definitions approach each other. For example, for $L = 75$, $r \in [1, 10]$ the linear fit to the dependence $\mathcal{U}(r)$ on $\frac{1}{r}$ gives $\mathcal{U}(r) \sim 0.97/r - 0.18$ while for $L = 100$, $r \in [1, 10]$ the fit is $\mathcal{U}(r) \sim 0.997/r - 0.155$. However, on lattices of the sizes we used the difference is important. Say, on the lattice 24^4 the fit is $\mathcal{U}(r) \sim 0.82/r - 0.35$ (for $r \in [1, 5]$). Thus, the values of the renormalized α_R extracted from (24) and (25) are significantly different from each other. Any of the two ways, (24) or (25), may be considered as the *definition* of the renormalized α on the finite lattice. And there is no particular reason to prefer the potential defined using the lattice Fourier transform of the Coulomb law in momentum space. Actually, our study shows that the single $1/r$ fit approximates \mathcal{V} much better. Therefore, we used it to extract α_R . This should be compared with the results of [12], where for similar reasons the single $e^{-\mu r}/r$ fit (instead of the lattice Yukawa fit) was used in order to determine the renormalized coupling constant in the $SU(2)$ Gauge-Higgs model. However, the fact that both definitions give values that differ from each other shows the limitation on the interpretation of our results and the importance of finite volume effects in our research.

4.4. Nambu monopole density and percolation probability

According to Eqs. (13, 14) the worldlines of the quantum Nambu monopoles could be extracted from the field configurations in two ways:

$$j_Z = \delta\Sigma = \frac{1}{2\pi} * d([dZ'] \bmod 2\pi) \quad (26)$$

and

$$j_A = \delta\Sigma = \frac{1}{2\pi} * d([dA] \bmod 2\pi). \quad (27)$$

The monopole density is defined as

$$\rho = \left\langle \frac{\sum_{\text{links}} |j_{\text{link}}|}{4L^4} \right\rangle, \quad (28)$$

where L is the lattice size (in lattice units).

In order to investigate the condensation of monopoles we use the percolation probability $\Pi(A)$. It is the probability that two infinitely distant points are connected by a monopole cluster (for more details of the definition see, for example, [35]).

Both $-j_A$ and $+j_Z$ describe the same physical object. However, this object may have a size that is larger than one lattice spacing. That's why the two different ways to extract the monopole trajectory may give different currents. The difference between the two currents is $j_Z - (-j_A) = j_Z + j_A$. Therefore, the density of $j_A + j_Z$ measures the degree of how j_A differs from $-j_Z$. In order to investigate the difference between the two definitions of Nambu monopole currents we use the quantity $\rho(j_A + j_Z)$, that is constructed using the current $j_Z + j_A$ as in (28).

4.5. Action density near monopole trajectories

The monopole worldline lives on the dual lattice. Each point of the worldline is surrounded by a three - dimensional hypercube of the original lattice. We measure the plaquette part of the action S_p^{mon} on the plaquettes that belong to those three-dimensional hypercubes (normalized by the number of such plaquettes). The excess of the plaquette action near monopole worldlines over the mean plaquette part of the action S_p is denoted by

$$\Delta S_p = \frac{1}{S_p}(S_p^{\text{mon}} - S_p). \quad (29)$$

Very roughly ΔS_p can be considered as measuring the magnetic energy (both $SU(2)$ and $U(1)$), which is carried by Nambu monopoles.

We also measure S_l^{mon} , which is the part of the action S_l^{mon} on the links of the original lattice that connect vertices of the two incident three-dimensional hypercubes mentioned above. The excess of this link action near monopole worldlines over the mean link part of the action S_l is denoted by

$$\Delta S_l = \frac{1}{S_l}(S_l^{\text{mon}} - S_l). \quad (30)$$

For the simplicity of the calculations we use only one of the 8 links that connect incident hypercubes.

4.6. Hypercharge monopoles

In addition to the Nambu monopoles we also investigated the behavior of some objects which are called hypercharge monopoles. Their worldlines are extracted from the hypercharge field θ in the following way:

$$j_Y = \frac{1}{2\pi} * d([d2\theta]_{\text{mod}2\pi}) \quad (31)$$

We also define their density according to the expression (28).

Actually, in the naive continuum limit hypercharge monopoles would have an infinite energy. They may appear only if one takes into account the finiteness of the ultraviolet cutoff. It occurs that they are mainly of interest in the strong coupling region, where the two considered lattice models appear to behave differently.

5. Numerical results

5.1. Phase diagram

The phase diagrams of the two models under consideration are presented in Fig. 1. At small values of the coupling constants the model with the gauge group $SU(2) \otimes U(1)/Z_2$ has already been investigated in our earlier paper [5]. The model with the gauge group $SU(2) \otimes U(1)$ was investigated in the paper [14] (also at small values of the coupling constants). The dashed vertical line represents the phase transition in the

$SU(2) \otimes U(1)$ -symmetric model (we call it further Model A). This is the confinement-deconfinement phase transition corresponding to the $U(1)$ constituents of the model. The same transition for the $SU(2) \otimes U(1)/Z_2$ -symmetric model (we call it model B) is represented by the solid vertical line. The dot-dashed horizontal line corresponds to the transition between the broken and symmetric phases of model A. The solid horizontal line represents the same transition in model B. Interestingly, in the $SU(2) \otimes U(1)/Z_2$ model both transition lines meet, forming a triple point. Much attention was paid to this fact in [5].

So, in both models there are three phases. The first one is situated in the left-hand side of the phase diagram. In this phase there are confinement-like forces both between the right-handed and the left-handed external fermions. However, due to the presence of the charged scalar field the string connecting external fermions is broken and the confining forces disappear at a certain distance (see, for example, [5]). In this phase both Nambu monopoles and hypercharge monopoles are condensed. The second phase is situated below the horizontal phase transition line and right to the vertical phase transition line. In this phase the confining forces are observed only between the left-handed fermions. The hypercharge monopoles are not condensed in this phase and their density falls sharply. For the detailed description of different phases of the $SU(2) \otimes U(1)/Z_2$ -symmetric model (including the properties of topological objects and static potentials) at small values of β see [5].

Real physics is commonly believed to be achieved within the phases of the two models situated in the right upper corner of Fig. 1. In this phase neither Nambu monopoles nor hypercharge monopoles are condensed. The confining-like forces are not observed here both between right-handed and left-handed fermions. The double-dotted-dashed vertical line on the right-hand side of the diagram represents the line, where the renormalized α is constant and equal to $1/128$. In order to draw the phase-transition lines at small values of β we use the results of [5] and [14]. These data have been checked using the observables listed in the previous section. In particular, the density of hypercharge monopoles appears to be very sensitive to the $U(1)$ confinement-deconfinement phase transition, while the density and percolation probability of Nambu monopoles feel the transition between the broken and symmetric phases. The position of the horizontal line for large values of β is obtained using mainly the percolation probability for the Nambu monopoles (which has been found to be an order parameter of the corresponding transition in the lattice Standard Model, with $SU(3)$ constituents included [7]). This position corresponds also to the maximum of the susceptibility $\chi = \langle H^2 \rangle - \langle H \rangle^2$. (See Fig. 6. We calculated the susceptibility using both definitions, Eqs. (19 and (20) for H .)

All simulations were performed on lattices of sizes 8^4 and 16^4 . Several points were checked using a lattice 24^4 . In general we found no significant difference between the mentioned lattice sizes.

5.2. Renormalized masses and couplings

In the region $\beta \in (10, 20)$, $\gamma \in (1, 2)$ we found no difference between the two versions of lattice electroweak theory. Therefore, we omit mentioning to what particular model the considered quantity belongs in this region of coupling constants.

The Z -boson masses is found to change very slowly with the variation of β . The dependence on γ seems to be stronger. M_Z in lattice units grows with the increase of γ .

For the calculation of the Z -boson mass we used lattices of sizes: $6^3 \times 12$, $8^3 \times 16$, $12^3 \times 24$, and $16^3 \times 24$. The dependence of the Z -boson correlator Eq. (17) on $r = x_0 - y_0$ is presented in Fig. 2 for $\gamma = 1$, $\beta = 15$ and a lattice $16^3 \times 24$. From this plot we extract the mass of the Z -boson to be 0.22 ± 0.02 . It is important to notice that we did not find any dependence of M_Z on lattice size.

At $\beta = 15$ we localize the position of the transition between the symmetric and broken phases of the model at $\gamma_c = 0.92 \pm 0.02$. The measured Z - boson mass for $\gamma \in [0.9, 0.94]$ is 0.21 ± 0.02 . So, we evaluate the Z - boson mass at the transition point to be $M_Z = 0.21 \pm 0.02$. The correspondent value of the ultraviolet cutoff (the inverse lattice spacing) is $\Lambda = 90 \text{ GeV}/M_Z = 430 \pm 40 \text{ GeV}$.

As for the Higgs boson mass, due to the insufficient statistics we cannot extract M_H from our data with reasonable accuracy. According to our (very rough) estimate at $\beta = 15$, $\gamma = 1$ we have $M_H/M_Z \sim 9 \pm 2$. This estimate is in agreement with the investigation of the $SU(2)$ Higgs model [10, 11, 12] performed near the transition point for the London limit of the Higgs potential and realistic β . Actually, as in [10] we made our estimate based on the consideration of the correlator for small “time” separation (≤ 3).

It was found in [12] that at larger distances a second mass parameter close to $2M_W$ contributes to the correlator. In our study the accuracy of measurements does not allow us to extract information from the H - H correlator for “time” separations ≥ 4 . Therefore, we do not see the signal of the two gauge-boson bound state. However, we do not exclude that it would appear if more statistics is collected and “time” separations ≥ 4 are explored.

In [12] in order to evaluate the Higgs boson mass in this situation the value of mass $\sim 2M_W$ was considered as the mass of the bound state of the two gauge bosons, and only the first mass in the given channel was interpreted as the Higgs boson mass. Actually, we do not see any reason to do so, and guess that the second mass in this channel may serve as the Higgs boson mass. However, this question must be investigated separately. Therefore we only claim here that the Higgs boson mass for our choice of initial parameters is larger than about $2M_W \sim 160 \text{ GeV}$, that could be the lowest mass in the given channel.

The renormalized coupling constant α is found to be close to the realistic value $\alpha(M_Z) = 1/128$ along the line represented in Fig. 1. In Fig. 3 the dependence of the potential for infinitely heavy right-handed leptons on $1/r$ is shown for $\gamma = 1$, $\beta = 15$. The renormalized α_R is extracted from this dependence. Actually, a linear dependence

is observed for $r \in [1, 6]$. Therefore we treat this constant as $\alpha_R(r/a) \sim \alpha_R(M_Z)$. In Fig. 4 we exhibit the dependence of $1/\alpha_R$ on β for fixed $\gamma = 1$. Here it should be mentioned that according to the subsection IV.C of the present paper, the definition of the renormalized α on the lattices of finite size suffers from lattice artifacts.

5.3. Nambu monopoles

We used both definitions of Nambu monopoles given in section 3. In Fig. 5 we show their density and percolation probability as a function of γ along the line of constant renormalized $\alpha_R = 1/128$. Interestingly, the density and percolation probability coincide here for the two mentioned definitions of Nambu monopole while the precise position of monopole trajectories differ by about 30%, i.e., we found that $2\rho(j_A + j_Z)/(\rho(j_A) + \rho(j_Z)) \sim 0.3$. This means that the physical Nambu monopole has a size larger than 1 in lattice units. Therefore the two different lattice definitions locate it sometimes differently.

It is clear from Fig. 5 that the percolation probability is the order parameter of the transition from the symmetric to the broken phase. We did not investigate the order of the transition. However, according to the previous investigations of the $SU(2)$ Higgs model [26] we expect that for our choice of the Higgs potential it could actually be a crossover.

In order to compare the position of the transition between the symmetric and broken phases with the point where the percolation probability vanishes, we investigated the susceptibility $\chi = \langle H^2 \rangle - \langle H \rangle^2$ extracted both from $H_Z = \sum_y Z_{xy}^2$ and $H_W = \sum_y |W_{xy}|^2$. The dependence of χ on γ along the line of constant $\alpha = 1/128$ is shown in Fig. 6.

The magnetic energy ΔS_p carried by a Nambu monopole is presented in Fig. 7. The excess of the link action near the monopole worldline ΔS_l is shown in Fig. 8. The behavior of both variables show that a quantum Nambu monopole may indeed be considered as a physical object.

5.4. Relation between the lattice model and continuum physics

The real continuum physics should be approached along the line of constant α_R , i.e., along the line of constant physics (at this point we omit consideration of θ_W and M_H). From our data it follows that the ultraviolet cutoff $\Lambda = a^{-1} = (90 \text{ GeV})/M_Z$ grows with decreasing γ along the line of constant physics. This dependence is not far from the tree-level estimate $\Lambda/\text{GeV} = 90/M_Z = 90\sqrt{\beta/\gamma} \cos\theta_W \sim 310/\sqrt{\gamma}$. It occurs that Λ is increasing slowly along this line with decreasing γ and achieves a value close to 430 ± 40 GeV at the transition point between the physical Higgs phase and the symmetric phase. (At $\beta = 15$ the transition occurs at $\gamma_c = 0.92 \pm 0.02$, where the Z boson mass in lattice units is evaluated to be $M_Z = 0.21 \pm 0.02$.) Therefore, we claim that up to finite volume artifacts the largest achievable value of the ultraviolet cutoff is around 430 ± 40 GeV if the potential for the Higgs field is considered in the London limit.

It is interesting to understand what happens with this maximal value of the ultraviolet cutoff if the Higgs potential would contain a finite scalar self coupling λ [9]. Then for the case of the $SU(2) \times U(1)/Z_2$ symmetric model we chose the action of the form

$$\begin{aligned}
 S = \beta \sum_{\text{plaquettes}} & \left((1 - \frac{1}{2} \text{Tr} U_p \cos \theta_p) + \frac{1}{2} (1 - \cos 2\theta_p) \right) + \\
 & - \gamma \sum_{xy} \text{Re}(\Phi^\dagger U_{xy} e^{i\theta_{xy}} \Phi) + \sum_x (|\Phi_x|^2 + \lambda(|\Phi_x|^2 - 1)^2), \quad (32)
 \end{aligned}$$

where Φ is the scalar doublet. Here $\gamma = 2\kappa$, where κ corresponds to the constant used in the investigations of the $SU(2)$ gauge Higgs model [15, 16, 17, 18, 19, 20, 21, 22, 23, 24, 25, 10, 11, 12]. The weak coupling expansion in lattice theory [13] gives the prediction that the maximal possible ultraviolet cutoff is achieved in lattice electroweak theory at infinite λ . Thus we expect that the largest achievable value of the ultraviolet cutoff for any λ should be close to the value 430 ± 40 GeV calculated in our present work. One can compare this result with that of the previous research (see Table 1).

We like to note, that from the point of view of perturbation theory the energy scale 1 TeV appears in the so-called hierarchy problem [2]. Namely, the mass parameter μ^2 for the scalar field receives a quadratically divergent contribution in one loop. Therefore, formally the initial mass parameter ($\mu^2 = -\lambda_c v^2$, where v is the vacuum average of the scalar field) should be set to infinity in such a way that the renormalized mass μ_R^2 remains negative and finite. This is the content of the so-called fine tuning. It is commonly believed that this fine tuning is not natural [2] and, therefore, the finite ultraviolet cutoff Λ should be maintained. From the requirement that the one-loop contribution to μ^2 is less than $10|\mu_R^2|$ one derives that $\Lambda \sim 1$ TeV.

Our lattice study demonstrates the following peculiar feature of electroweak theory. If we are moving along the line of constant $\alpha = 1/128$, then the Nambu-monopole density decreases with increasing γ (for $\gamma > 1$). Its behavior is approximated with a good accuracy by the simple formula:

$$\rho \sim e^{2.08 - 4.6\gamma}. \quad (33)$$

It is worth mentioning, that the monopole density given by (33) is expressed in lattice units. The density expressed in physical units may be defined as $\rho_c = \frac{\rho}{a^3}$, where a is the lattice spacing. It was mentioned above that the lattice spacing decreases with decreasing γ . Thus the Nambu monopole density expressed in physical units increases with decreasing a .

Naively one may think that the density (in lattice units) should decrease with increasing ultraviolet cutoff and the physical value of the density is achieved at the transition point. However, it occurs that the situation is inverse. Thus the density in physical units does not tend to a constant at $a \rightarrow 0$. Therefore, it is not clear how to extract the physical continuum density of Nambu-monopoles from the lattice data. In this connection it is also important to notice that we did not find any dependence of the monopole density on the lattice size.

6. On the difference between the considered lattice models

In the previous section we have seen that there exists no difference between the two lattice models with the gauge groups $SU(2) \times U(1)/Z_2$, and $SU(2) \times U(1)$ at realistic values of the coupling constants. However, such a difference clearly exists in the region of large coupling constants ($\alpha > 0.1$), where the phase diagrams of the two models do not coincide. In particular, this difference can be easily seen from the behavior of the hypercharge-monopole density (see Fig. 9, where the dependence on β is shown for $\gamma = 1.5$). In the same figure the density of Nambu monopoles (defined through the Z' field) is presented as well. It is clear that the two kinds of monopoles behave differently in the two models.

The explanation of this fact may be related to the possible appearance of the unification of fundamental interactions at the energy scale Λ of about 1 TeV. Namely, it has been shown in [36] that if TeV physics is described by a simply connected unified gauge group (as in Petite Unification Models [37, 38]), then the following relation exists between the additional discrete symmetry of the Standard Model and the monopole content of the theory, which describes TeV physics: If the electroweak theory has the gauge group $SU(2) \times U(1)/Z_2$, then there are topologically stable monopoles in the unified theory, which are composed of electroweak fields (when seen from large enough distances). From those monopoles the hypercharge magnetic flow

$$\int_c 2B^\mu dx^\mu \sim 2\pi \quad (34)$$

should emanate. Therefore, at low energies they may be identified with the hypercharge monopoles, defined in Eq. (31). Such objects do not appear if the gauge group of electroweak theory is $SU(2) \times U(1)$. Those topologically stable objects have masses of the order of Λ/α . At realistic values of the coupling constant they could not be observed at low energies within the electroweak theory with the ultraviolet cutoff Λ , as their masses appear to be much larger than the cutoff. However, if one would imagine that the coupling constant α in our world becomes close to unity, then the mass of such objects becomes comparable to Λ . If so, their density in the case of the $SU(2) \times U(1)/Z_2$ -symmetric model must exceed considerably the same density calculated within the $SU(2) \times U(1)$ model.

Exactly this happens in our models, where the ultraviolet cutoff Λ is estimated to be of the order of 400 GeV. The naive expression Λ/α for the mass of hypercharge monopole (in the $SU(2) \times U(1)/Z_2$ -symmetric model) gives values comparable to Λ in the region of couplings presented in the figure, where α is found to be of the order of 0.1. It still remains larger than the cutoff, but we should remember that the classical evaluation of mass may be renormalized via quantum fluctuations. Thus, we can see that the density of hypercharge monopoles in the $SU(2) \times U(1)/Z_2$ model indeed exceeds the one of the $SU(2) \times U(1)$ model in the region of small β (the bare value of α is $1/(4\pi\beta)$).

7. Conclusions

In this paper we investigated lattice electroweak theory numerically at realistic values of the fine structure constant and the Weinberg angle. We considered the potential for the Higgs field in the London limit, i.e., for infinite bare scalar self coupling.

We found that the two definitions of the theory (with the gauge groups $SU(2) \otimes U(1)/Z_2$ and $SU(2) \otimes U(1)$, respectively) do not lead to different predictions at these values of the couplings. However, the corresponding models behave differently at unphysically large values of α . The main difference is in the behavior of the so-called hypercharge monopoles, which would become the Z_2 monopoles of the unified theory, if the latter has a simply connected gauge group.

On the phase diagram of the considered lattice model a line can be drawn, where the renormalized fine structure constant is close to its realistic value $\frac{1}{128}$. It should be remembered, though, that in order to draw the true line of constant physics (where the Higgs mass and the renormalized Weinberg angle are constant as well) one must vary the bare Weinberg angle and the bare scalar self coupling.

Our investigation of the line of constant renormalized α for the infinite bare self coupling of the Higgs field allows us to draw the conclusion that values of lattice spacings smaller than about $(430 \pm 40 \text{ GeV})^{-1}$ cannot be achieved in principle for this choice of the potential for the Higgs field (at least, for the considered lattice sizes). It would be important, therefore, to consider finite values of the scalar self couplings and investigate finite volume artifacts in order to understand whether there is a maximal value of the ultraviolet cutoff in the electroweak theory (that is not related to a Landau pole in renormalized α and λ).

Actually, we suppose that at the point of the transition the line of constant physics (corresponding to the Higgs phase) stops and another line of constant physics begins (that corresponds to the unphysical symmetric phase). Although usually the transition is thought to be a crossover, we see that the physical content of the theory is changed drastically at the transition. Namely, Nambu monopoles appear to be condensed in the symmetric phase. So, these objects dominate in the dynamics of this phase of the theory. This, of course, contradicts all observable data. Thus the points of the symmetric phase cannot be associated with real physics. The percolation probability of Nambu monopoles appears as an order parameter for this transition. Therefore we conclude, that the given transition may belong to the class of the transitions of the so-called Kertesz type (see, for example, [39, 40]). That's why one may suppose that the position of this percolation transition may not correspond precisely to the position of the transition determined with the aid of other physical quantities. However, according to our results, for example, the position of the percolation transition coincides within statistical errors with the position of the maximum of the susceptibility extracted from the Higgs boson creation operator (see Figs. 5 and 6).

It is worth mentioning, that the gauge boson mass does not vanish at the transition point. So, it differs from zero in the symmetric phase of the theory, not only in

the physical Higgs phase. This is in accordance with the previous numerical data [9, 26, 15, 16, 17, 18, 19, 20, 21, 22, 23, 24, 25, 10, 11, 12]. For pure $SU(2)$ theory (the limit $\gamma \rightarrow 0$) the situation is more complicated: The gluon propagator contains a mass parameter, but the dependence on the momentum is not consistent with the usual mass pole (see, for example, [41]).

We have found that the Nambu monopole density on the lattice increases with increasing ultraviolet cutoff. Although we obtain this result for fixed bare Weinberg angle and infinite bare scalar self coupling, we expect that it should remain unchanged in the full theory with variable θ_W and λ . Thus we conclude, that the conventional electroweak theory is not able to predict the density of Nambu monopoles. This is, however, not a surprise because the Standard Model should be considered as a finite cutoff theory. According to common lore and in accordance with our numerical results discussed above, the Standard Model cannot describe nature at energies above 1 TeV. On the other hand, in [1] the Nambu monopole mass was (roughly) estimated to be in the TeV region. This rough estimate, however, is obtained based on the classical consideration of monopole configurations. In quantum theory the density of monopoles is defined by the balance of entropy and self energy. We found that the density of the monopoles approaches a value of the order of 0.1 (in lattice units) near the transition to the unphysical phase of the theory. Therefore, it is natural to suppose that the self energy of these objects decreases when the transition is approached within the Weinberg - Salam model. We indeed observe the decrease of the action near monopole trajectories (see Fig.(7) and Fig (8)). So, we expect that the value of mass evaluated near the transition should be significantly less than the classical value calculated in [1]. On the other hand, it is natural to suppose that the monopole mass approaches its classical value deep in the Higgs phase. There the Nambu monopole currents are not observed in our study as it should when one looks for an object with a mass above 1 TeV at energies of the order of 100 GeV.

To conclude, the description of Nambu monopole physics based on the lattice Weinberg - Salam model with finite ultraviolet cutoff seems to us incomplete. The correct nonperturbative description may, therefore, be obtained within the lattice theory that involves the description of TeV - scale physics. Nevertheless, on the basis of electroweak theory only we are able to reach the conclusion that Nambu monopoles appear as real physical objects: Our numerical results show that the action density near the Nambu monopole worldlines exceeds the density averaged over the lattice in the physical region of the phase diagram. This confirms the classical consideration of [1], where corresponding classical configurations were found to carry energy. Another important piece of information about the structure of the lattice Weinberg - Salam model comes from the consideration of the percolation of monopole currents. The percolation probability is found to be an order parameter for the transition between the symmetric and broken phases. In the unphysical symmetric phase of the model Nambu monopoles are condensed, which means that this phase of the lattice model indeed cannot be associated with the real continuum physics.

A.I.V. and M.A.Z. kindly acknowledge the hospitality of the Department of Physics and Astronomy of the Vrije Universiteit, where part of this work was done. This work was partly supported by RFBR grants 05-02-16306, 07-02-00237, and 08-02-00661, RFBR-DFG grant 06-02-04010, by Federal Program of the Russian Ministry of Industry, Science and Technology No 40.052.1.1.1112, by Grant for leading scientific schools 843.2006.2.

- [1] Y. Nambu, Nucl.Phys. B **130**, 505 (1977);
Ana Achucarro and Tanmay Vachaspati, Phys. Rept. **327**, 347 (2000); Phys. Rept. **327**, 427 (2000).
- [2] J.A. Casas, J.R. Espinosa, and I. Hidalgo, hep-ph/0607279.
- [3] F. del Aguila and R. Pittau, Acta Phys. Polon. B **35**, 2767 (2004).
- [4] B.L.G. Bakker, A.I. Veselov, and M.A. Zubkov, Phys. Lett. B **583**, 379 (2004);
- [5] B.L.G. Bakker, A.I. Veselov, and M.A. Zubkov, Yad. Fiz. **68**, 1045 (2005).
- [6] B.L.G. Bakker, A.I. Veselov, and M.A. Zubkov, Phys. Lett. B **620**, 156 (2005)
- [7] B.L.G. Bakker, A.I. Veselov, and M.A. Zubkov, Phys. Lett. B **642**, 147 (2006).
- [8] J. Jersak, C.B. Lang, T. Neuhaus, G. Vones, Phys.Rev. D **32**,2761 (1985).
H.G. Evertz, J. Jersak, C.B. Lang, T. Neuhaus, Phys. Lett. B **171**, 271 (1986). H.G. Evertz,
V. Grosch, J. Jersak, H.A. Kastrup, T. Neuhaus, D.P. Landau, J.L. Xu, Phys. Lett. B **175**, 335 (1986).
- [9] I. Montvay, Nucl. Phys. B **269**, 170 (1986)
- [10] W. Langguth, I. Montvay, and P. Weisz, Nucl. Phys. B **277**, 11 (1986)
- [11] W. Langguth and I. Montvay (DESY), Z.Phys.C **36**, 725 (1987).
- [12] Anna Hasenfratz and Thomas Neuhaus, Nucl. Phys. B **297**, 205 (1988)
- [13] I. Montvay, BNL Gauge Theor.Symp. (1986) 235; Nucl. Phys. B 293 (1987) 479.
- [14] R. Shrock, Phys. Lett. B **162**, 165 (1985); Nucl. Phys. B **267**, 301 (1986).
- [15] F. Csikor, Z. Fodor, and J. Heitger Phys. Rev. Lett. **82**, 21 (1999); Phys. Rev. D **58**, 094504 (1998); Nucl. Phys. Proc. Suppl. **63**, 569 (1998).
- [16] F. Csikor, Z. Fodor, and J. Heitger, Phys. Lett. B **441**, 354 (1998).
- [17] F. Csikor, Z. Fodor, J. Hein, A. Jaster, and I. Montvay, Nucl. Phys. B **474**, 421 (1996).
- [18] Joachim Hein (DESY) and Jochen Heitger, Phys. Lett. B **385**, 242(1996).
- [19] F. Csikor, Z. Fodor, J. Hein, J. Heitger, A. Jaster, and I. Montvay, Nucl. Phys. Proc. Suppl. **53**, 612 (1997).
- [20] Z. Fodor, J. Hein, K. Jansen, A. Jaster, and I. Montvay, Nucl. Phys. B **439**, 147 (1995).
- [21] F. Csikor, Z. Fodor, J. Hein, and J. Heitger, Phys. Lett. B **357**, 156 (1995).
- [22] F. Csikor, Z. Fodor, J. Hein, K. Jansen, A. Jaster, and I. Montvay, Nucl. Phys. Proc. Suppl. **42**, 569 (1995).
- [23] F. Csikor, Z. Fodor, J. Hein, K. Jansen, A. Jaster, and I. Montvay, Phys. Lett. B **334**, 405 (1994).
- [24] Y. Aoki, F. Csikor, Z. Fodor, and A. Ukawa, Phys. Rev. D **60**, 013001 (1999); Nucl. Phys. Proc. Suppl. **73**, 656 (1999).
- [25] Y. Aoki, Phys. Rev. D **56**, 3860 (1997).
- [26] M. Gurtler, E.-M. Ilgenfritz, and A. Schiller, Phys. Rev. D **56**, 3888 (1997).
K. Rummukainen, M. Tsypin, K. Kajantie, M. Laine, and M. Shaposhnikov, Nucl. Phys. B **532**, 283 (1998);
Yasumichi Aoki, Phys. Rev. D **56**, 3860 (1997);
N. Tetradis, Nucl. Phys. B **488**, 92 (1997);
B. Bunk, Ernst-Michael Ilgenfritz, J. Kripfganz, and A. Schiller (BI-TP-92-46), Nucl. Phys. B **403**, 453 (1993);
B. Bunk, Ernst-Michael Ilgenfritz, J. Kripfganz, and A. Schiller (BI-TP-92-12), Phys. Lett. B **284**, 371 (1992).
- [27] Thomas A. DeGrand, Doug Toussaint, Phys. Rev. D **22**, 2478 (1980).
- [28] J. Ranft, J. Kripfganz, G. Ranft, Phys.Rev.D **28**, 360 (1983).
- [29] Wolfgang Franzki, John B. Kogut, M.P. Lombardo, Phys. Rev. D **57**, 6625 (1998).
- [30] M.N. Chernodub, F.V. Gubarev, E.M. Ilgenfritz, and A. Schiller, Phys. Lett. B **434**, 83 (1998);
M.N. Chernodub, F.V. Gubarev, E.M. Ilgenfritz, and A. Schiller, Phys. Lett. B **443**, 244 (1998).
- [31] M.N. Chernodub, JETP Lett. **66**, 605 (1997)
- [32] C. Gardner, J. Harvey, Phys. Rev. Lett. **52**, 879 (1984);
Tanmay Vachaspati, Phys. Rev. Lett. **76**, 188 (1996);

- Hong Liu, Tanmay Vachaspati, Phys. Rev. D **56**, 1300 (1997).
- [33] K.S. Babu, I. Gogoladze, and K. Wang, Phys. Lett. B **570**, 32 (2003);
K.S. Babu, I. Gogoladze, and K. Wang, Nucl. Phys. B **660**, 322 (2003).
- [34] M.I. Polikarpov, U.J. Wiese, and M.A. Zubkov, Phys. Lett. B **309**, 133 (1993).
- [35] B.L.G. Bakker, A.I. Veselov, and M.A. Zubkov, Phys. Lett. B **471**, 214 (1999).
- [36] M.A. Zubkov, Phys. Lett. B **649**, 91 (2007).
- [37] Andrzej J. Buras, P.Q. Hung, Phys. Rev. D **68**, 035015 (2003).
- [38] Andrzej J. Buras, P.Q. Hung, Ngoc-Khanh Tran, Anton Poschenrieder, and Elmar Wyzomirski,
Nucl.Phys. B **699**, 253 (2004);
Mehrddad Adibzadeh and P.Q. Hung, hep-ph/0705.1154.
- [39] D. Stauffer, A. Aharony, "Introduction to percolation theory", (Taylor & Francis, London, 1994).
- [40] M.N. Chernodub, Phys. Rev. Lett. **95**, 252002 (2005).
- [41] O. Oliveira, P. J. Silva, E.-M. Ilgenfritz, A. Sternbeck, arXiv:0710.1424

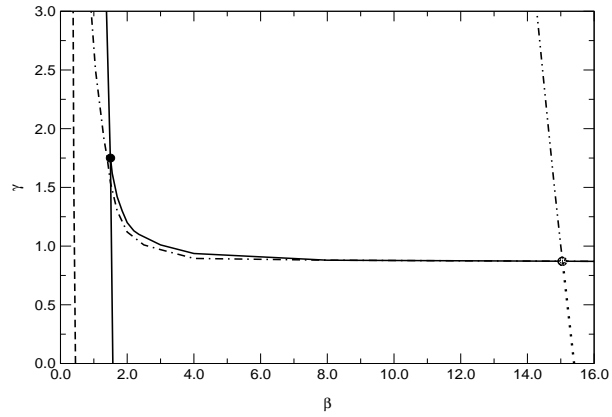


Figure 1. The phase diagrams of the models in the (β, γ) -plane. The dashed line and the dot-dashed line represent phase transitions in the $SU(2) \otimes U(1)$ model. The transitions for the $SU(2) \otimes U(1)/Z_2$ -symmetric model are represented by the solid lines. The double-dotted-dashed vertical line on the right-hand side of the diagram represents the line, where the renormalized α is constant and equal to $1/128$.

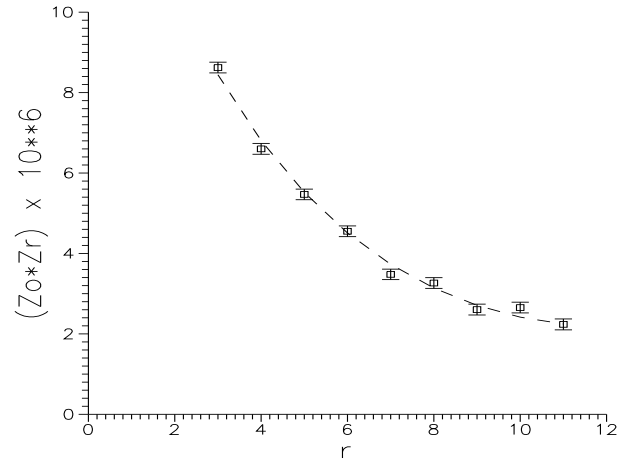


Figure 2. $\frac{1}{4R^6} \sum_{\bar{x}, \bar{y}} \sum_{\mu} \langle Z_x^{\mu} Z_y^{\mu} \rangle$ as a function of $r = |x_0 - y_0|$. Here $R = 16$ is the lattice size in “space” direction.

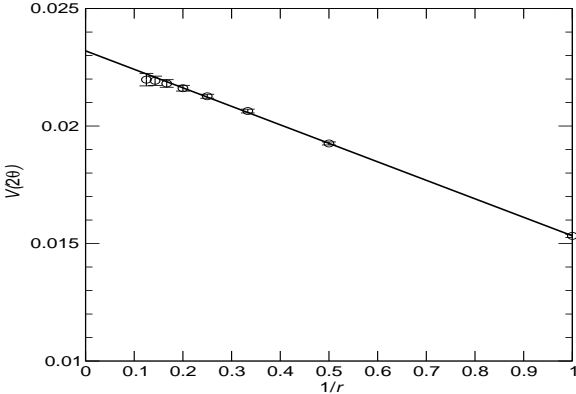


Figure 3. Potential for right-handed leptons as a function of $1/r$ for $\beta = 15, \gamma = 1$.

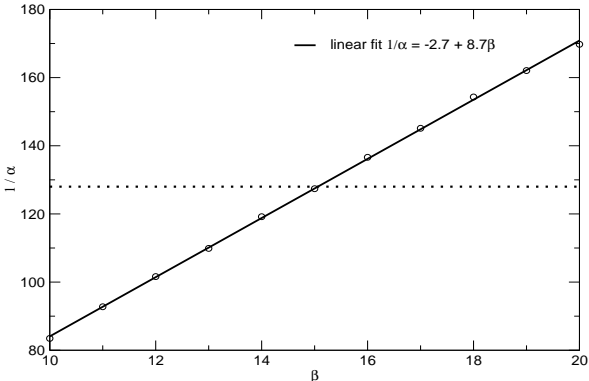


Figure 4. Renormalized coupling $1/\alpha_R$ as a function of β for $\gamma = 1$.

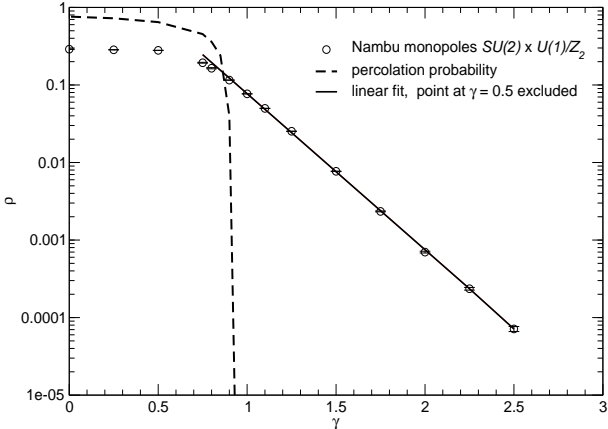


Figure 5. Nambu monopole density and percolation probability as a function of γ along the line of constant $1/\alpha_R = 128$.

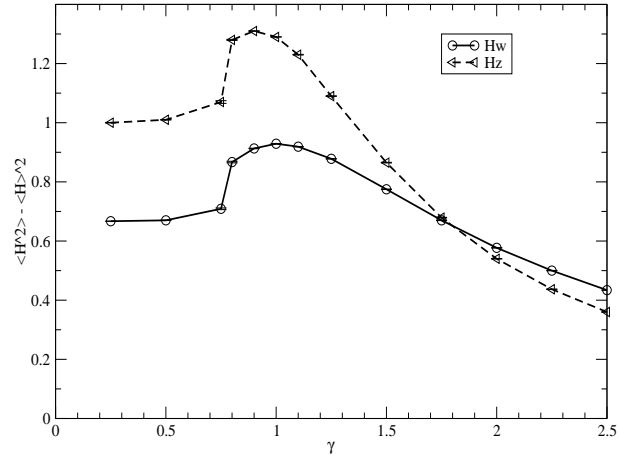


Figure 6. Susceptibility $\chi = \langle H^2 \rangle - \langle H \rangle^2$ along the line of constant $1/\alpha_R = 128$. Here H_W is the operator defined in (19), while H_Z is defined by (20).

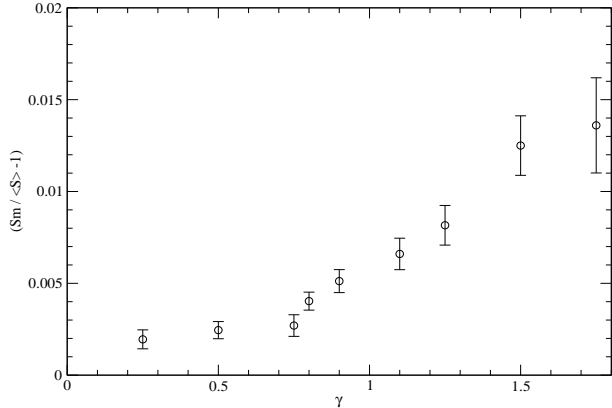


Figure 7. Excess of the plaquette action near monopole trajectories along the line of constant $1/\alpha_R = 128$.

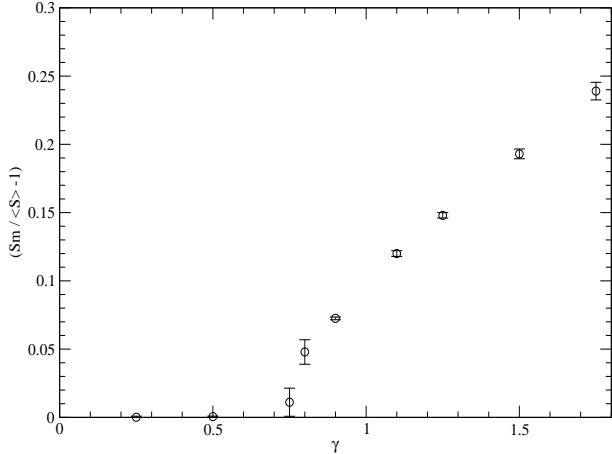


Figure 8. Excess of the link action near monopole trajectories along the line of constant $1/\alpha_R = 128$.

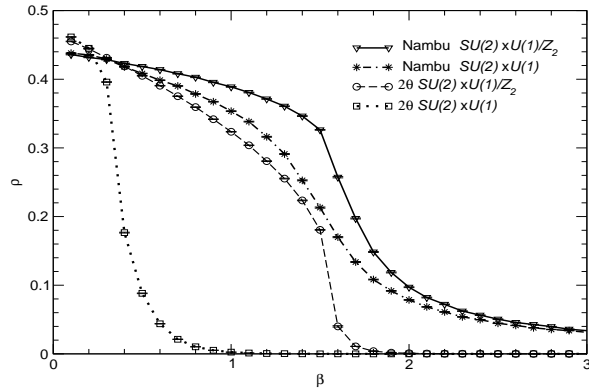


Figure 9. Densities of hypercharge monopoles and Nambu monopoles (extracted from Z') as a function of β for $\gamma = 1.5$ for both models.